Biochimica et Biophysica Acta 1844 (2014) 1145–1152

Contents lists available at ScienceDirect

Biochimica et Biophysica Acta

journal homepage: www.elsevier.com/locate/bbapap

Differential role of molten globule and protein folding in distinguishing unique features of botulinum neurotoxin

Raj Kumar, Roshan V. Kukreja, Shuowei Cai, Bal R. Singh *

Department of Chemistry and Biochemistry, University of Massachusetts, Dartmouth, MA 02747, USA

ARTICLE INFO

Article history:
Received 23 October 2013
Received in revised form 15 February 2014
Accepted 17 February 2014
Available online 22 February 2014

Keywords:
Fluorescence
Enzyme catalysis
Protein folding
Protein denaturation
Protein conformation

ABSTRACT

Botulinum neurotoxins (BoNTs) are proteins of great interest not only because of their extreme toxicity but also paradoxically for their therapeutic applications. All the known serotypes (A-G) have varying degrees of longevity and potency inside the neuronal cell. Differential chemical modifications such as phosphorylation and ubiquitination have been suggested as possible mechanisms for their longevity, but the molecular basis of the longevity remains unclear. Since the endopeptidase domain (light chain; LC) of toxin apparently survives inside the neuronal cells for months, it is important to examine the structural features of this domain to understand its resistance to intracellular degradation. Published crystal structures (both botulinum neurotoxins and endopeptidase domain) have not provided adequate explanation for the intracellular longevity of the domain. Structural features obtained from spectroscopic analysis of LCA and LCB were similar, and a PRIME (PReImminent Molten Globule Enzyme) conformation appears to be responsible for their optimal enzymatic activity at 37 °C. LCE, on the other hand, was although optimally active at 37 °C, but its active conformation differed from the PRIME conformation of LCA and LCB. This study establishes and confirms our earlier finding that an optimally active conformation of these proteins in the form of PRIME exists for the most poisonous poison, botulinum neurotoxin. There are substantial variations in the structural and functional characteristics of these active molten globule related structures among the three BoNT endopeptidases examined. These differential conformations of LCs are important in understanding the fundamental structural features of proteins, and their possible connection to intracellular longevity could provide significant clues for devising new countermeasures and effective therapeutics.

1. Introduction

Botulinum neurotoxins (BoNTs), produced by Gram-positive bacteria, *Clostridium botulinum*, are the most toxic substances known. BoNTs are responsible for human and animal botulism. The lethal effect of BoNT is mediated by intracellular cleavage of SNARE (soluble *N*-ethylmaleimide-sensitive factor attachment proteins receptor) [1] protein in presynaptic nerve endings, which are essential for neuroexocytosis [2]. Cleavage of SNARE proteins results in the blockage of acetylcholine release at nerve–muscle junctions resulting in flaccid muscle paralysis, and eventually respiratory collapse. Paradoxically, while BoNT is a very toxic potential warfare agent, it also has a wide range of medical applications related to neuromuscular disorders, including blepharospasm, hyperhidrosis, and cervical dystonia [3–5]. BoNT-based products are also being used for cosmetic purposes, such as removal of wrinkles [6].

Eight distinct serotypes (A-H) of BoNT are produced by *Clostridium botulinum* as single chain 150 kDa molecules, which are changed to dichain molecules by proteolytic cleavage at the Lys–Ala peptide bond, either by proteolytic enzymes in tissue or in bacterial cytosol. This cleavage creates a 100 kDa heavy chain (HC) and a 50 kDa light chain (LC) connected via a disulfide bond and non-covalent interactions [7,8]. Heavy chain can be hydrolyzed into two 50 kDa domains, C-terminus binding domain (H_c) and N-terminus translocation domain (H_N). BoNT is composed of three domains: binding domain, translocation domain, and catalytic or endopeptidase domain. These three domains, respectively, allow BoNT to bind to cell surface receptors, pass through the endosomal membrane, and cleave the protein(s) involved in the synaptic vesicle docking. [1]. BoNT/A, BoNT/B, and BoNT/E neurotoxins are known to cause human botulism, and cleave the SNAP-25 (BoNT/A and E; 9) and VAMP (BoNT/B) [10] component of SNARE. While all the serotypes have similar domain organization and function, and show only immunological distinction [10], duration of their intracellular action (longevity) and potency vary substantially. BoNT/A, BoNT/B, and BoNT/E intoxication is persistent for about 180 days, 90 days, and 30 days, respectively [9,11,12]. Persistence of the BoNT/A intoxication

Abbreviations: BoNT, botulinum neurotoxin; PRIME, Pre-imminent molten globule enzyme; CD, circular dichroism; MG, molten globule; SNARE, soluble NSF attachment protein receptor, NSF, *N*-ethylmaleimide-sensitive factor; VAMP, vehicle associated membrane protein

* Corresponding author at: Botulinum Research Centre, Institute of Advanced Sciences, 78-540, Faunce Corner Road, North Dartmouth, MA 02747, USA. Tel.: +1 508 992 2042; fax: +866 709 1689.
E-mail address: bsingh@inads.org (B.R. Singh).

http://dx.doi.org/10.1016/j.bbapap.2014.02.012
1570-9639/

is because of the stability of its catalytic domain, the light chain, inside neuronal cells [13,14]. The basis of differential stability of light chains of different BoNT serotypes is critical to develop countermeasures against botulism, and more effective therapeutic products. Possible reasons for the long term persistence of BoNT/A light chains could be phosphorylation and ubiquitination [15,16], which may depend on the structural and conformational state of the light chains.

Crystal structures of BoNT LCs suggest a high level of similarity in secondary and tertiary structures, as well as identical active site motif (HEXXH) and other active site participating residues (Y, R and E), which have little to offer as an explanation for the differential intracellular behavior of these molecules. Since light chains are the catalytic moieties of BoNTs, which upon entering the cell are responsible for the toxicity in neuronal cells, it is important to examine the structural features of the light chains of different BoNT serotypes. Comparison of LC structure of BoNT/A, BoNT/B, and BoNT/E may provide us clues to understand the differential behavior of these molecules.

In this work, we have examined the structural features of BoNT/A, B and E light chains to look for the elements of the PRIME structure, which has already been established for the BoNT/A light chain [17]. We have addressed the question as to whether the PRIME structure is a common structural feature involved in the function of these molecules. Our observations suggest that the BoNT/B light chain exhibits the PRIME structure which is responsible for its optimal activity at 37 °C, similar to BoNT/A LC. However, existence of PRIME conformation is not clearly visible for BoNT/E LC, despite its optimal activity at 37 °C.

2. Materials and methods

2.1. Expression and purification of BoNT/A, BoNT/B and BoNT/E light chains

All the light chains were purified on Ni^{2+} column according to the method described earlier [18]. BoNT/A and BoNT/B light chains were purified in phosphate buffer (10 mM sodium phosphate pH 8.0, containing 300 mM NaCl) but due to the solubility problem BoNT/E was purified in Tris-buffer (50 mM Tris pH 8.0, containing 500 mM NaCl). Prior to conducting experiments, all light chains were dialyzed in 10 mM phosphate buffer, pH 7.3, containing 150 mM NaCl and 1 mM DTT.

2.2. CD spectroscopy

CD spectra were measured at 25 °C on Jasco J715 CD spectrophotometer (Jasco Inc., Easton NJ) equipped with a Peltier type temperature controller (Model PTC-348 W). For secondary and tertiary structure measurements by CD spectral analysis in far-UV and near-UV regions, respectively, 0.2–0.3 mg/ml and 0.5 mg/ml concentrations of LC were used. For secondary structure analysis, spectra were recorded between 250 nm and 190 nm, and for tertiary structure, spectra were recorded between 310 nm and 250 nm. Spectral recording was carried out at a speed of 20 nm/min with a response time of 8 s, using cuvettes with different pathlength for far-UV (1 mm) and near-UV (1 cm). A total of three scans were recorded and averaged to increase the signal to noise ratio. The final spectra were obtained after correcting the buffer contribution. Secondary structure content was determined by using the Jasco secondary structure estimation program, which is based on the algorithm of Yang et al. [19].

For thermal denaturation experiments, protein was heated to a given temperature, and the CD spectrum was recorded after incubating the sample at that temperature for 5 min.

For thermal unfolding of the secondary structure, CD signal at 222 nm was monitored with a heating rate of 1 °C/min between 25 °C and 90 °C. High concentration of protein required for the near-UV CD signal resulted in protein aggregation at high temperatures. Therefore, it was not possible to monitor tertiary structure changes with CD.

2.3. Urea denaturation of BoNT endopeptidase

Recombinant full length LCA, LCB and LCE were dialyzed against the phosphate buffer (10 mM sodium phosphate, 150 mM NaCl, 1 mM dithiotritol, pH 7.3), and diluted to a fixed concentration of LC (0.2 mg/ml) by a series of varying urea concentrations (at least 0.5 M apart) from a 10 M stock urea solution yielding a final urea concentration in the sample between 0 and 8 M. All the mixtures were equilibrated for at least 2 h at 25 °C before recording CD spectra. CD spectrum was recorded between 250 nm and 190 nm.

Circular dichroism (CD) spectra were recorded in the far-UV region at 25 °C under similar conditions as described above, and the data was plotted for signal at 222 nm for each LC–urea concentration.

2.4. Fluorescence spectroscopy

Fluorescence measurements of BoNT LCs were carried out using the ISS K2 fluorimeter. Protein solutions (0.1 mg/ml) were excited at 280 and 295 nm, and emission spectra were recorded between 310 and 400 nm. Experiments were carried out in 10 mm fluorescence cuvette. Excitation and emission slits width were fixed at 4 nm.

Thermal denaturation of tertiary structure was monitored by fluorescence. For measuring thermal denaturation by fluorescence we used the ratio of F_{351}/F_{316} and F_{351}/F_{306} for LCB and LCE, respectively. F is fluorescence intensity, and numbers represent wavelengths of emission. Samples were heated from 25 to 90 at a rate of 1 °C/min. Excitation wavelength for thermal denaturation experiment was 280 nm.

2.5. Second derivative UV spectroscopy

Absorption spectra of LC dissolved in buffer (10 mM sodium phosphate pH 7.3, containing 150 mM NaCl and 1 mM DTT) were recorded between 225 and 330 nm on a Simadzu UV spectrophotometer, attached with a water bath to control temperature. The spectra were derivatized to the second order having 0.2 nm resolution and delta lambda. The ratio of a (an arithmetic sum of the negative $d^2A/d^2\lambda$ at 284 nm and positive $d^2A/d^2\lambda$ at 289.5 nm) and b (an arithmetic sum of the negative at 291 nm and the positive at 294 nm) was measured at different temperatures.

2.6. ANS binding

ANS (1,8-anilinonapthalenesulfonate) is a dye whose fluorescence is strongly quenched by water, and undergoes a dramatic increase in fluorescence intensity when it binds to hydrophobic regions of a protein molecule. ANS binding was performed for BoNT/B and BoNT/E LCs. ANS was titrated into 1 ml of 1 μM of protein solution in 10 mM sodium phosphate pH 7.3, containing 150 mM NaCl and 1 mM DTT, in a 1 cm path length cuvette. BoNT/B and BoNT/E LC each was titrated to 70 μM and 80 μM ANS, respectively, to reach the fluorescence saturation. Excitation wavelength was 370 nm, and emission spectra were recorded from 410 nm to 510 nm. Excitation and emission slit widths were fixed at 4 and 8 nm, respectively. Fluorescence intensities were measured at different temperatures, after the solution was incubated for 5 min at each temperature.

2.7. Endopeptidase assay

BoNT/B LC (LCB) was assayed for endopeptidase activity by using Vamptide (OBZ/DNP; List Biological, Campbell, CA) as its substrate. This peptide is intramolecularly quenched by FRET (fluorescence resonance energy transfer). The FRET assay was carried out at a given temperature with excitation at 321 nm and emission 418 nm. Excitation and emission slit widths were fixed at 4 nm. Before adding substrate, LCB was incubated at the designated temperature for 30 min. For the endopeptidase activity of LCB, the concentrations of the Vamptide and

LCB used were 6 μM and 100 nM, respectively, dissolved in an assay buffer (10 mM sodium phosphate, containing 150 mM NaCl and 1 mM DTT, pH 7.3). The enzyme reaction was carried out for 60 min with continuous monitoring of the fluorescence signal.

BoNT/E LC (LCE) was assayed for endopeptidase activity using fluorescence peptide substrate, SNAPEtide (List Biological Inc., CA) as its substrate. Since enzyme activity curve was saturating faster with 100 nM LCE, we used 50 nM LCE for the determination of the endopeptidase activity. The temperature effect on the endopeptidase activity of LCE was examined by incubating 6 μM SNAPEtide with 50 nM LC at the designated temperature for 10 min in an assay buffer (10 mM sodium phosphate buffer, 150 mM NaCl, and pH 7.3). Before adding SNAP Etide, 50 nM LCE was incubated for 30 min at the designated temperature. The plate was read in a SpectraMax M5 microplate reader (Molecular devices, Menlo Park, CA, USA) using an excitation wavelength of 320 nm and an emission wavelength of 420 nm. The endopeptidase activity of BoNT/E was estimated by comparing the fluorescence intensities of the control SNAPEtide with that of the cleaved SNAPEtide.

3. Results and discussion

3.1. General comparison of the secondary and tertiary structure in the solution

Our aim was to compare the structure of endopeptidase domain of BoNT/A, B and E. Secondary and tertiary structures of the globular protein can be probed by far-UV and near-UV CD measurements, respectively [20]. A CD spectrum in the far-UV region recorded between 250 nm and 190 nm allows estimation of the secondary structure of a protein. BoNT/A and BoNT/B LC spectra (Fig. 1A) recorded at the same concentration of protein showed similar mean residue weight ellipticity at 222 nm and 208 nm, which is indicative of the similar α-helical content of these proteins. In contrast, the BoNT/E LC spectrum showed higher ellipticity at 208 nm than at 222 nm (Fig. 1A), which is indicative of lower α-helicity in this protein compared to BoNT/A and BoNT/B LCs. This observation is in agreement with the secondary structure estimation using the algorithm of Yang et al. [19]. BoNT/A LC (LCA) had α-helicity of 27.1% ± 0.9%, BoNT/B LC (LCB) had 24.2% ± 0.9% and BoNT/E LC (LCE) had 21.3% ± 0.6%. Combined β-sheet and β-turn contents of BoNT/A, BoNT/B, and BoNT/E LCs were 39.7%, 42.0%, and 47.7%, respectively (Table 1).

The CD spectrum in the near-UV region, between 310 and 250 nm, provides information on the tertiary structure of proteins. While there is a remarkable similarity in the near-UV CD spectra of LCA and LCB, showing a major negative maxima at 280 nm, with minor shoulders at 264 and 269 nm, the near-UV CD spectrum of LCE, in contrast, showed major positive CD maxima at 280 nm and 287 nm (Fig. 1B). In addition, the LCE spectrum showed the usual negative maxima at 264 and 269 nm. LCA and LCB exhibited insignificant differences in their CD spectra, with a mean residue ellipticity of about -6.22×10^1 deg cm^2/dmol at 280 nm. On the other hand, (LCE) had molar ellipticity of about $+2.64 \times 10^1$ deg cm^2/dmol at 280 nm (Fig. 1B). In the near-UV CD, a broad minimum at 280 nm is indicative of asymmetry around Tyr and minima around 263 nm and 269 nm is indicative of environment around Phe. The near-UV CD results appear to indicate that peptide segments containing Phe residues are topographically located in similar environments in all the three LCs examined. However, signals belonging to Tyr (280 and 287 nm) and Trp (287 nm) suggest that the environmental orientation of peptide segments with these residues in LCA and LCB on one hand and LCE on the other is dramatically different. Since all three LCs have about 18 Tyr residues each, it is difficult to pinpoint the origin of the CD signal to assign the differences. However, LCB and LCE each have a single Trp residue in their sequences, whereas LCA has two Trp residues. This makes it possible to identify peptide segments, which would be clearly distinct in the three proteins. In view of an earlier report, where it was argued that the absence of CD bands

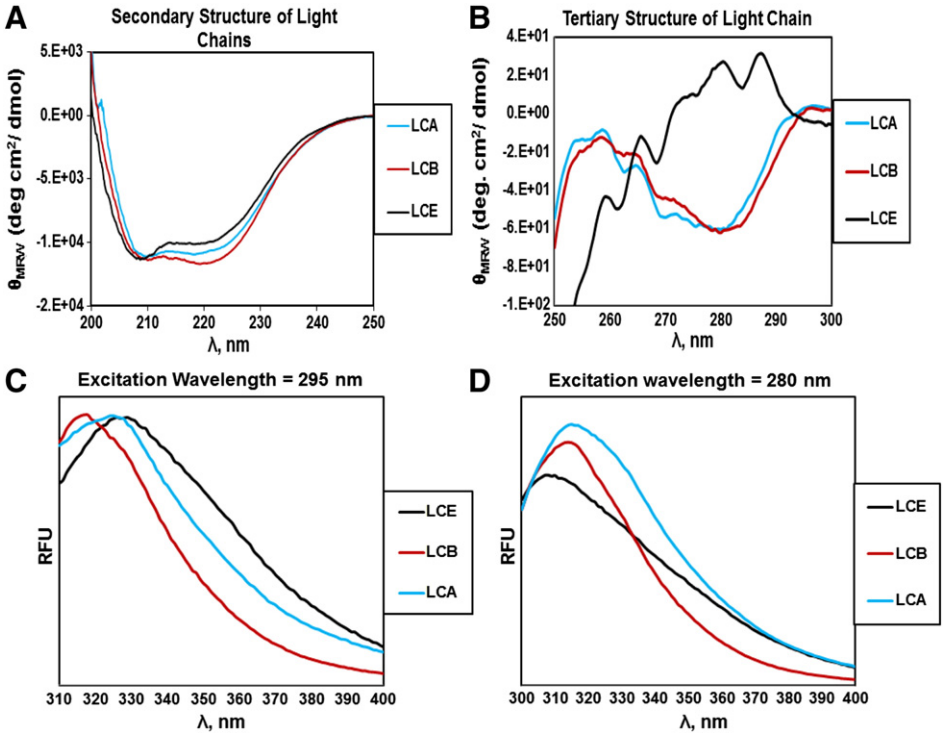

Fig. 1. (A) Far-UV spectra of LCA (blue), LCB (red) and LCE (black) dissolved (0.15–0.30 mg/ml) in sodium phosphate buffer, pH 7.3, containing 150 mM NaCl and 1 mM DTT. The spectral contribution from the buffer was subtracted from protein spectra. (B) Near-UV spectra of LCA, LCB and LCE (0.5 mg/ml) dissolved in sodium phosphate buffer, pH 7.3, containing 150 mM NaCl and 1 mM DTT. The spectral contribution from the buffer was subtracted from protein spectra. All spectral recordings were carried out at 25 °C. Fluorescence spectra of LCA (blue), LCB (red) and LCE (black). Excitation wavelength was 295 nm (C) and 280 nm (D). RFU is the relative fluorescence intensity. Protein concentration was 0.1 mg/ml, and spectra were recorded at 25 °C.

Table 1
Secondary structure content of BoNT/A LC, BoNT/B LC and BoNT/E LC determined by using the Yang et al. [19] algorithm.

	α-Helix (%)	β-sheet + turns (%)	Random coil (%)
BoNT/A LC	27.07 ± 0.93	39.57 ± 1.27	33.37 ± 0.21
BoNT/B LC	24.20 ± 0.90	42.03 ± 0.96	33.93 ± 1.85
BoNT/E LC	21.30 ± 0.61	46.67 ± 3.79	32.00 ± 2.34

belonging to Trp residues in LCA was a result of CD signals from Trp-43 and Trp-118 cancelling each other [21], it is notable that both LCE and LCB have their Trp residues in the same general location (at amino acid position 39 and 43, respectively). The fact that the near-UV CD spectra of LCA and LCB are nearly identical, it would seem that Trp-43 residues in their respective proteins are located in a conformationally symmetric segment. Trp-118 of LCA is in a flexible segment of the protein based on the crystal structure analysis (PDB ID: 2ISE), and thus is not expected to exhibit CD signal. However, given the fact that Trp fluorescence is even more blue shifted (316 nm) in LCB in comparison to LCA (324 nm), it is likely that the peptide segments containing Trp-42(LCA)/Trp-43(LCB) are in a hydrophobic region, and thus in a rigid conformation. This further reinforces the notion that there is a conformational symmetry around Trp-42(LCA)/Trp-43(LCB), and this contributes to the loss of the Trp CD signal. In LCE Trp-39 fluorescence was red shifted (329 nm), which indicates that Trp-39 (LCE) is in relatively less hydrophobic environment compared to LCA and LCB. However, moderately positive CD signal at 287 nm in LCE suggests that the Trp-39 segment in LCE exists in a significantly asymmetric conformation compared to the equivalent Trp residues of LCA and LCB.

Tertiary structures of all the three proteins were also monitored by fluorescence spectroscopy. Protein fluorescence is generally excited either at 280 or 295 nm. Emission maxima of LCA, LCB, and LCE are 324 nm, 316 nm, and 329 nm, respectively, for an excitation wavelength of 295 nm (Fig. 1C), which is indicative of a well folded structure of at least the Trp containing segments of these proteins. This difference in emission maxima also indicates the difference in the topography of Trp in these proteins. Trp in LCB is in a relatively more hydrophobic environment than LCA or LCE. With the excitation at 280 nm, emission maxima for LCA, LCB and LCE were at 316 nm, 315 nm, and 306 nm, respectively, showing maximum blue shift for LCE although there was a significant shift in LCA (Fig. 1D), leaving the LCB least affected by the excitation wavelength. In general, Tyr fluorescence is effectively transferred to tryptophan through FRET [22]. This is not the case with LCE, and to a certain extent with LCA, whereas in the case of LCB Tyr is able to effectively transfer its energy to tryptophan, indicating differential tertiary structural organization in LCE compared to LCA and LCB. This finding is consistent with our conclusions from the near-UV CD data presented earlier (*vide supra*).

3.2. Temperature-dependent enzymatic and structural changes

To investigate comparative optimum temperatures for enzymatic activity and functional stability of LCA, LCB and LCE at different temperatures, we determined the endopeptidase activity of LCB and LCE, and compared with the activity of LCA (17; Fig. 2 and SM Fig. 2) at different temperatures. The substrate for LCB was Vamptide, a synthetic peptide with a native cleavage site, and the substrate for LCE was SNAPEtide. It was observed that both 100 nM of LCB and 50 nM of LCE were optimally active at 37 °C. LCE loses its activity beyond 37 °C but remained active even up to 50 °C, retaining about 44% activity. LCB, on the other hand, lost its activity beyond 37 °C, with total loss at 50 °C (Fig. 2).

Temperature-dependent structural changes were monitored with CD signals at 222 and 280 nm, which showed sigmoidal curves, indicating stability of secondary and tertiary structures (Fig. 3A and B). The transition curves based on temperature-dependent CD signal at 222 nm indicated an apparent melting temperature of 48 °C for LCA,

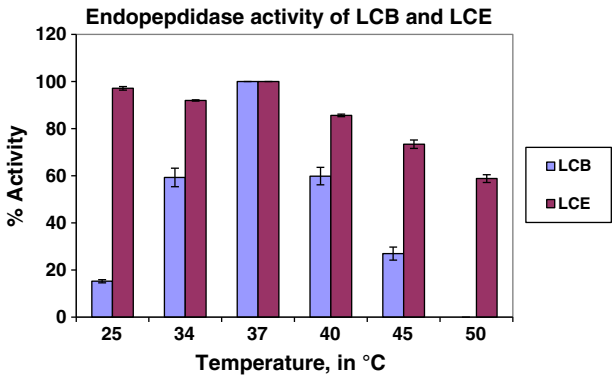

Fig. 2. Endopeptidase activity of LCB and LCE at different temperatures. Endopeptidase activity of 100 nM of LCB at different temperatures using 6 μM of fluorescence substrate (Vamptide, OBZ/DNP; List Biological, Campbell, CA) monitored with FRET signal. Cleavage was monitored with excitation wavelength of 321 nm and emission wavelength of 418 nm. Endopeptidase activity of 50 nM of LCE at different temperatures using 6 μM of fluorescence substrate (SNAPEtide, OBZ/DNP; List Biological, Campbell, CA). Cleavage was monitored with excitation wavelength of 321 nm and emission wavelength of 418 nm. All the reactions of LCB and LCE were performed in 10 mM sodium phosphate buffer, pH 7.3, containing 150 mM NaCl and 1 mM DTT. Before adding substrate, both the proteins were incubated for 30 min at designated temperature. Percent activity was calculated by assuming 100% activity at 37 °C.

52 °C for LCB, and 54 °C for LCE (Fig. 3A). Because of aggregation, it was not possible to record thermal transition curves for monitoring tertiary structural stability at 280 nm for LCB and LCE by circular dichroism spectroscopy. So we measured temperature dependent denaturation of the tertiary structure of LCA, LCB and LCE by measuring the ratio of fluorescence intensity at 351 nm and intensity at emission maxima of the proteins. Excitation wavelength was 280 nm. Melting temperature of LCA, LCB and LCE measured by fluorescence was 47 °C (Fig. 3B). Thermal denaturation of secondary and tertiary structures of all the light chains suggested that each of these proteins loses its tertiary structure before losing the secondary structure, indicating possibility of the existence of molten globule intermediate conformation (SM Fig. 3A, B and C). Notably, transitions of secondary and tertiary structures of LCA [17] and LCB from native to denatured states were sharp, and appeared to have a cooperative transition, whereas in case of LCE the transition was extended, indicating non-cooperative thermal denaturation (Fig. 3A and B).

Temperature dependent unfolding of tertiary structure of LCB and LCE was also analyzed by monitoring the exposure of Tyr residue by the second derivative UV spectroscopy, and compared against LCA. The second derivative of UV absorption spectra of LCB and LCE, both dissolved in phosphate buffer (10 mM sodium pH 7.3, 150 mM NaCl and 1 mM DTT), are shown in Fig. 4. The spectral region of interest is 280–300 nm. LCB had two negative bands at 285 nm and 293 nm, with positive bands at 291 nm and 295 nm. In the case of LCE negative peaks were at 285 nm and 293 nm, with positive bands at 288 nm and 294 nm. Second derivative spectra for both the proteins were obtained at different temperatures in the 25 °C to 45 °C range. The a/b ratio was calculated for both the proteins to determine the exposure of Tyr residue at each of these temperatures. The a/b ratios of LCB at 25 °C and 42 °C were, 1.59 ± 0.11 and 0.85 ± 0.02, respectively. Transition point of the decrease was at 37 °C (1.11 ± 0.21). The a/b ratios for LCE at 25 °C and 45 °C were, 2.09 ± 0.07 and 0.83 ± 0.04, respectively. Transition point for LCE was significantly higher at 42 °C (1.40 ± 0.09). The a/b ratio of LCA was similar to LCB (17; Fig. 4). With increasing temperature there was no significant change in a/b ratio of LCA, but at 37 °C there was a marked decrease in the a/b ratio, which indicated the lower exposure of Tyr residue. Transition point of LCA was also 37 °C. Fig. 4 shows the normalized data of LCA, LCB and LCE, which shows similar patterns of the a/b ratio for LCA, LCB, and shows significant difference patterns from that of LCE. It was difficult to measure the ratio accurately

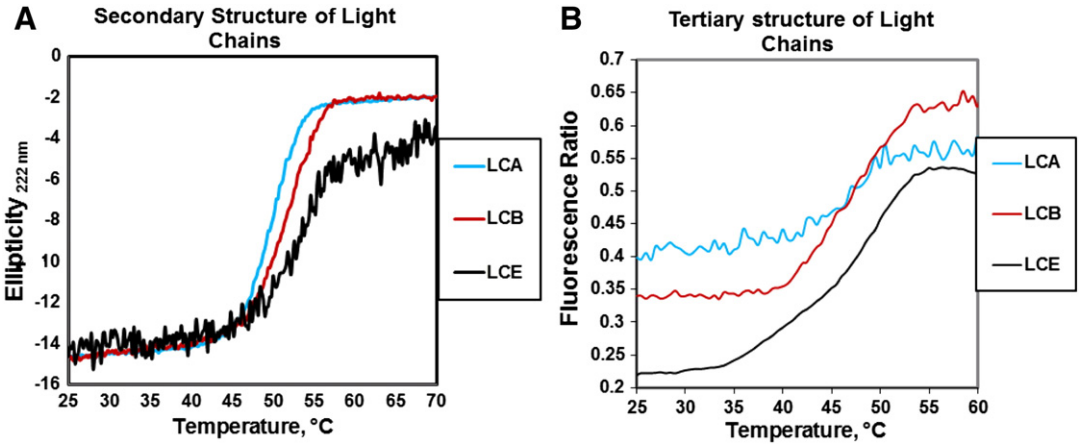

Fig. 3. (A) Thermal denaturation monitored for the secondary structure of LCA (blue), LCB (red) and LCE (black). All the proteins were dissolved in 10 mM sodium phosphate, pH 7.3, containing 150 mM NaCl and 1 mM DTT. Samples were heated at a rate of 1 °C/min. Thermal unfolding of protein secondary structure was monitored by continuously recording CD signal at 222 nm as a function of temperature. (B) Thermal unfolding of the tertiary structure of the protein was monitored by plotting the ratio of fluorescence intensity at 351 nm and 316 nm for LCA (blue) and LCB (red), and the ratio of intensity at 351 nm and 306 nm for LCE (black; B), as a function of temperature. Excitation wavelength for all the proteins was 280 nm.

after 42 °C and 45 °C for LCB and LCE, respectively, because of the increase in noise due to aggregation of the proteins. The decrease in a/b ratio is attributed to the lesser exposure of Tyr residues, which may be due to refolding. This observation may in part suggest a conformational change (especially in the vicinity of Tyr residues) of LCA and LCB at 37 °C compared to 25 °C. Since aggregation also increases with temperature, it may suggest that interactions between protein molecules increases because of exposure of hydrophobic residues and formation of tight packed structures. This could reduce the a/b ratio as observed in Fig. 4. In the case of LCE, a/b ratios at 37 °C and 25 °C were similar, making it difficult to draw any definitive conclusion about the conformational change in LCE at 37 °C compared to 25 °C.

3.3. Differential folding of LCA, LCB, and LCE probed by urea denaturation

We analyzed unfolding of the light chain (LCA, LCB, and LCE) secondary structure in urea by monitoring the CD signals at 222 nm, which is a measure of the α-helicity of a molecule. The denaturation of LCA by urea is shown in Fig. 5. With increasing concentration of urea, LCA showed two intermediates, I_1 and I_2. This experiment was repeated with lower concentrations of LCA, which shows a similar trend, suggesting that the intermediates are formed due to molecular folding, and not due to the aggregation of the protein [23]. LCA ellipticity at 222 nm gradually decreases until 3.75 M, and then starts increasing up to 5 M, followed by a further decrease in the signal (Fig. 5). So, I_1 is at 3.75 M urea and I_2 is at 5 M urea. Spectra of BoNT/A light chain incubated in urea solution were recorded (Fig. 5), which clearly showed that I_1 does not have any secondary structure, whereas I_2 has native like secondary structure [23]. In contrast, LCB and LCE have different urea denaturation curves (Fig. 5). LCE has a two-state denaturation, showing a steady decrease in CD signal with increasing urea concentration. LCB, on the other hand, has substantial deviation from the two-state denaturation, resembling a three-state model. It shows steady decrease in CD value at 222 nm until the urea concentration is 3.5 M, and no additional change in CD signal with further increase in urea concentration between 3.5 M and 5.5 M urea, followed by steady decrease in CD signal to reach the lowest signal at 8 M urea.

According to crystal structures, all the light chains have similar domain organizations and folding (PDB ID: 2ISE, 1F82, 1T3A). However, the above data suggests that the folding behavior of LCA, LCB and LCE seen in the solution is not possible to observe in the static crystal structure. It is possible that, in the solution, either domain organization or environments around these domains are not similar in all of the light chains. Each of the BoNT LCs belongs to a family of Zn^{2+} metalloproteases. As a characteristic of this family, Zn^{2+} is coordinated by two histidine residues of His-Glu-X-X-His, and a water molecule which is bonded to the glutamate residue of the motif and a distal Glu residue downstream in the primary sequence [24]. BoNT endopeptidase

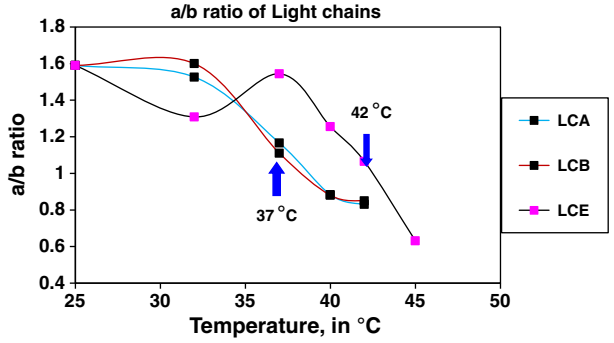

Fig. 4. Temperature change in the a/b ratio of LCA (blue), LCB (red), and LCE (black). a denotes an arithmetic sum of the negative $d^2A/d^2\lambda$ at 284 nm and positive $d^2A/d^2\lambda$ at 289.5 nm and b denotes an arithmetic sum of the negative at 291 nm and the positive at 294 nm. LCB and LCE were dissolved (0.2 mg/ml) in 10 mM sodium phosphate buffer, pH 7.3, containing 150 mM NaCl and 1 mM DTT. The a/b ratio of LCA (taken from Kukreja and Singh [17]) was overlapped with the a/b ratio of LCB and LCE for comparison.

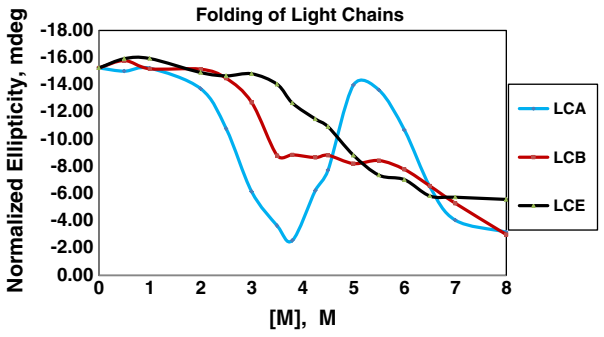

Fig. 5. Urea denaturation of LCA (blue), LCB (red) and LCE (black) as monitored by ellipticity at 222 nm. A quantity of 0.2 mg/ml of each protein was dissolved in 10 mM sodium phosphate buffer, pH 7.3, containing 150 mM NaCl, 1 mM DTT and different concentrations of urea (0–8 M). Prior to measurement protein solution was incubated for 2 h. All measurements and incubations were performed at 25 °C.

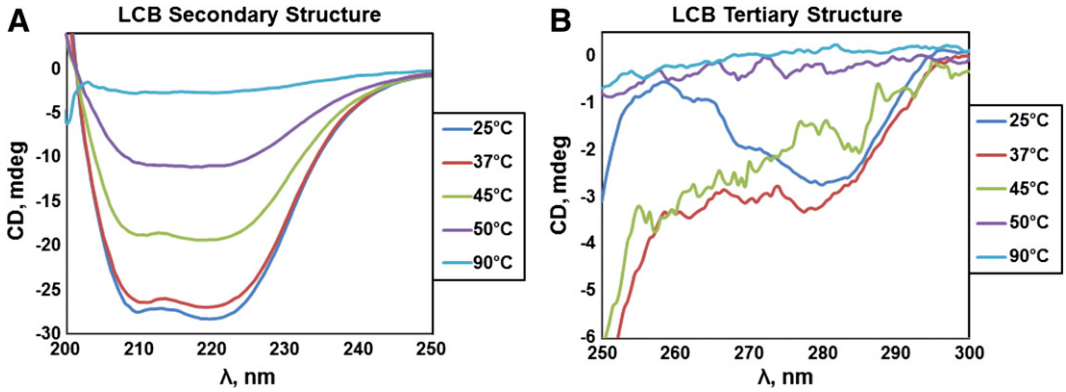

Fig. 6. (A) Far-UV CD spectra of LCB (0.2 mg/ml) dissolved in 10 mM sodium phosphate, pH 7.3, containing 150 mM NaCl and 1 mM DTT at 25 °C, 37 °C, 45 °C, 50 °C and 90 °C. (B) Near-UV CD spectra of LCB (0.5 mg/ml) dissolved in 10 mM sodium phosphate, pH 7.3, containing 150 mM NaCl and 1 mM DTT at 25 °C, 37 °C, 45 °C, 50 °C and 90 °C.

displays several unique characteristics such as extreme exclusivity, recognition, and specificity for its substrate. Role of tertiary structure is critical for this unique feature of BoNT endopeptidase [25–28]. The solved three-dimensional structures of BoNT LCs already have not been able to provide a convincing molecular explanation of differential substrate specificity as well as intracellular longevity. Co-crystal structure of BoNT/A LC and its truncated substrate is available [29], and it revealed the role of two exosites in addition to the active sites of the endopeptidases. We suspect that the three-dimensional folding of LCA, LCB, and LCE, including accessibility and dynamics of exosites, may hold clues to the understanding the unique specificity of BoNT endopeptidases.

3.4. PRIME conformation and molten globule of BoNT/B and BoNT/E light chain

Molten globule (MG) of an enzyme is an intermediate state; it conserves the native like secondary structure, but has less tightly packed protein interiors [30]. The semi-flexible structure of molten globule state allows hydrophobic groups to be exposed to water, which can be probed by hydrophobic dyes such as ANS. The loss of tertiary structure, while still maintaining the secondary structure, is a characteristic of the molten globule state. PRIME conformation is defined as pre-molten globule structure, where the enzyme is optimally active [17]. This conformational state of a protein has secondary structure similar to native state, but tertiary structure is more expanded compared to native state, although more compact than the molten globule state.

In this study, we monitored secondary and tertiary structures of LCB and LCE at different temperatures (25 °C to 90 °C) by CD spectroscopy. For secondary structure, ellipticity at 37 °C of LCB and LCE protein was the same as the ellipticity at 25 °C (Figs. 6 and 7). At 50 °C and 222 nm, LCB loses about 39% of ellipticity (Fig. 6A) and LCE loses about 50% of ellipticity (Fig. 7A). The tertiary structure monitored with near-UV CD signals indicates complete loss of tertiary structure at 50 °C at least for LCB (Fig. 6B). For LCE, the CD signals although turning negative from positive, still retain significant values, suggesting its refolding. This may be relevant to the observation that LCE remains enzymatically active up to 50 °C (Figs. 2 and 7A and B). Nevertheless, loss of tertiary structure in LCB and existence of flexible tertiary structure with significant secondary structure in LCE at 50 °C indicate the presence of the molten globule conformational state in both the proteins. The near-UV spectrum of LCB at 37 °C indicates increased mobility of peptide bonds in the vicinity of Phe and Tyr, whereas peptide bonds in the vicinity of Trp are still in the rigid part of the protein. So, the near-UV spectrum of LCB at 37 °C indicates a different conformational state compared to 25 °C. In the case of LCE, near-UV CD spectrum at 37 °C indicates lowering of the positive signal of Tyr and Trp compared to 25 °C. It is not clear whether lowering of the CD signal is due to the opening of structure or the loss of chirality of aromatic amino acids (Fig. 7B). Notably, no aggregation was observed at 37 °C, suggesting that the loss of signal is due to conformational change. We suggest that the signal change is due to the conformational change, leading to loss of chirality of aromatic amino acid residues. In the case of LCE, the 37 °C signal is less positive than 25 °C which suggests that LCE refolds, a conclusion which is also supported by the a/b ratio change (Fig. 4). The a/b ratio of LCE at 32 °C was lower than that of 25 °C, but interestingly at 37 °C the a/b ratio was similar to 25 °C. It is possible that the conformational state of LCE at 37 °C and 25 °C is different, and only the microenvironment around hydrophobic residues is similar, as reflected by similar a/

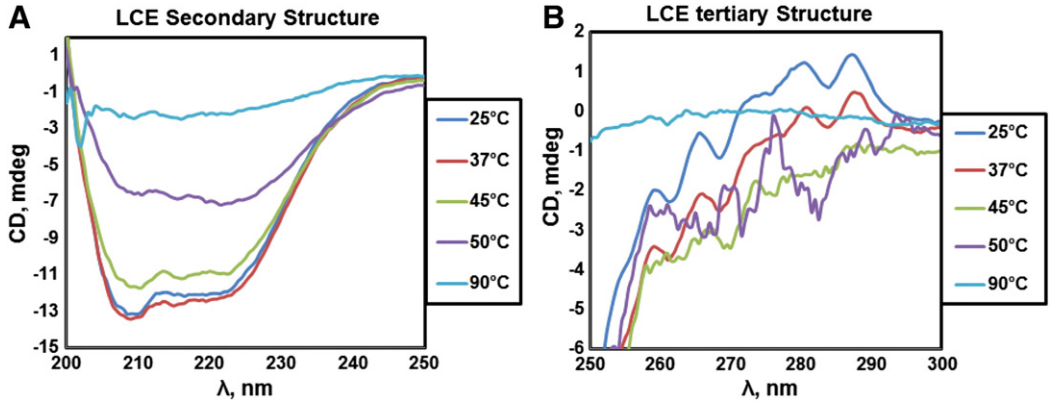

Fig. 7. (A) Far-UV CD spectra of LCE (0.2 mg/ml) dissolved in 10 mM sodium phosphate, pH 7.3, containing 150 mM NaCl and 1 mM DTT at 25 °C, 37 °C, 45 °C, 50 °C and 90 °C. (B) Near-UV CD spectra of BoNT/E LC (0.5 mg/ml) dissolved in 10 mM sodium phosphate, pH 7.3, containing 150 mM NaCl and 1 mM DTT at 25 °C, 37 °C, 45 °C, 50 °C and 90 °C.

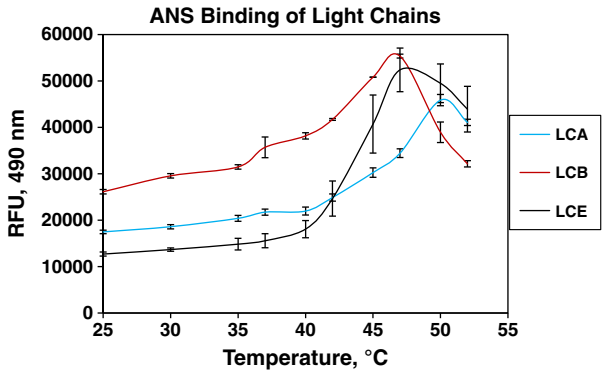

Fig. 8. Fluorescence intensity of ANS bound to LCA (blue, A; taken from Kukreja and Singh [17]) and overlap fluorescence intensity of ANS bound LCB (red) and LCE (black) as a function of temperature. Fluorescence emission was recorded at 490 nm for an excitation wavelength of 370 nm.

b ratio. These observations definitely suggest conformational changes in LCE at 37 °C compared to 25 °C, but it is difficult to make any conclusions based on the data of tertiary structure acquired by the near UV-CD and second derivative UV.

To further confirm the temperature-induced molten globule structure of both the proteins, we monitored ANS fluorescence as a function of temperature using optimum molar ANS to protein ratio of 70:1 and 80:1 for LCB and LCE, respectively. The ANS fluorescence reaches maximum at 47 °C for both the proteins, indicating optimal binding, the point at which both proteins virtually have less tertiary structures but sufficient amount of secondary structures. Thus, both LCB and LCE exist in a molten globule conformation at 47 °C (Figs. 6, 7 and 8). The ANS binding of LCB showed a small bump at 37 °C, which may be due to an expanded conformation of LCB. Notably, this is the temperature where this enzyme is optimally active. A similar observation was made by Kukreja and Singh [17] in the case of LCA (Fig. 8 and SM Fig. 1). The LCB enzyme was about 25% active at 45 °C, and completely lost its activity at 50 °C (Fig. 2). In the case of LCE, ANS binding showed a similar graph, but the bump at 37 °C was not observed. However, LCE was about 45% active at 50 °C (Fig. 2 and SM Fig. 2).

The above observations suggested the existence of a temperature-induced molten globule state for LCB. ANS binding (showing a shoulder in ANS binding at 37 °C), denaturation experiments monitored with CD, intrinsic fluorescence signals (showing differences in melting temperatures of secondary and tertiary structures), and second derivate spectroscopy (showing Tm for the tertiary structure at 37 °C) suggest the existence of an intermediate state of LCB at 37 °C, which is more expanded than the conformational state of enzyme at 25 °C and exhibits optimal activity (Figs. 2 and 8). This state is more densely packed than the molten globule state of LCB. This new intermediate state has a secondary structure similar to the conformational state at 25 °C, but the tertiary structure in this conformational state is comparatively more flexible. This intermediate state has similar structural and functional characteristics as the LCA PRIME conformation [17].

Secondary and tertiary structural analysis of LCE suggests the existence of molten globule state at 47 °C, which is also optimally active enzymatically (with full length substrate, SM Fig. 1). The only other example of an optimally active molten globule enzyme known is BoNT/A toxin [24]. It is notable that BoNT/E itself is maximally active from 45 °C to 50 °C [31], which may reflect a maximally active molten globule. However, unlike LCB, it was difficult to demonstrate the existence of a PRIME conformational state of LCE despite LCE being also optimally active at 37 °C. At 37 °C, there was no apparent differential secondary and tertiary structures, and the hallmark bump in ANS binding curve was absent (Fig. 8). In the absence of the PRIME conformation of LCE, other conformational features, which may allow its interaction with unique substrate and subsequent enzymatic activity, need to be identified.

Existence of molten globule as one of the intermediate states in protein folding is already established in other proteins [32,33]. This state is induced by temperature, pH, or osmolytes, and such conformational change is also linked to reduction of disulfide bonds [24,34,35]. In many cases protein–protein interactions also lead to this state of protein conformation. In recent years, pre-molten globule and molten globule states have also been demonstrated to be involved in biological functions [36,37]. However, no proteins other than BoNTs have been shown to exist in optimally active molten globule or PRIME conformational states. Endopeptidase domains of BoNT/A [17], BoNT/B, and BoNT/E exist as temperature-induced molten globule intermediate states. In this work, we also established the existence of a biologically active PRIME structure in the endopeptidase domain of BoNT/B, but not in that of BoNT/E. This PRIME conformational state is another unique intermediate state, which has an optimal binding affinity and activity of a protein, and it exists as between native state and molten globule state.

4. Conclusion

In conclusion, this study advances our earlier finding that an optimally active molten globule or related protein structures (PRIME) exist for the most poisonous poison, botulinum neurotoxin. There are substantial variations in the structural and functional characteristics of these active structures among the three BoNT endopeptidases examined. Existence of PRIME conformation in at least two different proteins advances the idea of the existence of this conformation in other proteins. Differential features of PRIME conformation in the three BoNT endopeptidases may be relevant to their specificity with substrates and their survival intracellularly. Finally, a proper understanding of the structural coordinates of active PRIME structures will be relevant to the design and development of antidotes against botulinum neurotoxins.

Acknowledgements

This work was supported in part by the US Army Medical Research Activity (Grant USAMRAA-W81XWH-08-P-0705), and the National Institutes of Health (Grant 1U01A1078070-01). We thank Mr. Stephen Riding for preparing the protein samples. We also thank the anonymous reviewers whose comments have helped us to improve the quality of the paper.

References

[1] G. Schiavo, M. Matteoli, C. Montecucco, Neurotoxins affecting neuroexocytosis, Physiol. Rev. 80 (2000) 717–766.
[2] B.R. Singh, Intimate details of the most poisionous poision, Nat. Struct. Biol. (Aug. 7 2000) 617–619.
[3] M.F. Brin, M.F. Lew, C.H. Adler, C.L. Comella, S.A. Factor, J. Jankovic, C.O. Brain, Neurobloc in type-A resistant cervical dystonia, Neurology 53 (1999) 1439–1447.
[4] K.M. Land, L.W. Cheng, Botulinum neurotoxin: a deadly protease with applications to human medicine, Current Research, Technology and Education Topics in Microbiology and Microbial Biotechnology, 2010. 965–971.
[5] K.R. Aoki, Botulinum toxin: a successful therapeutic protein, Curr. Med. Chem. 11 (2004) 3085–3092.
[6] K. Beer, J.L. Cohen, A. Carruthers, Cosmetic Use of Botulinum Toxin A, Cambridge University Press, 2007, pp. 328–348.
[7] J. Strotmeir, S. Gu, S. Jutzi, S. Mahrhold, J. Zhou, A. Pich, T. Eichner, H. Bigalke, A. Rummel, R. Jin, T. Binz, The biological activity of botulinum neurotoxin type C is dependent upon novel types of ganglioside binding sites, Mol. Microbiol. 81 (2011) 143–156.
[8] M. Montal, Botulinum neurotoxin: a marvel of protein design, Annu. Rev. Biochem. 79 (2010) 591–617.
[9] A. Pickett, K. Perrow, Towards new uses of botulinum toxins as a novel therapeutic tool, Toxins 3 (2011) 63–81.
[10] L.L. Simpson, A.B. Maksymowych, J.B. Park, R.S. Bora, The role of the interchain disulfide bond in governing the pharmacological actions of botulinum toxin, J. Pharmacol. Exp. Ther. 306 (2004) 857–864.

[11] M. Adler, J.E. Keller, R.E. Sheridan, S.S. Deshpande, Persistence of botulinum neurotoxin A demonstrated by sequential administration of serotypes A and E in rat EDL muscle, Toxicon 39 (2001) 233–243.
[12] J.O. Dolly, K.R. Aoki, The structure and model of different botulinum Toxins, Eur. J. Neurol. 13 (2006) 1–9.
[13] J.E. Keller, E.A. Neale, G. Oyler, M. Adler, Persistence of botulinum neurotoxin in cultured spinal cord cells, FEBS Lett. 456 (1999) 137–152.
[14] M. Adler, D.A. McDonald, L.C. Sellin, G.W. Parker, Effect of 3,4- diaminopyridine on rat extensor digitorum longus muscle paralyzed by local injection of botulinum neurotoxin, Toxicon 34 (1996) 237–249.
[15] A.V.F. Montiel, J.M. Canaves, B.R. DasGupta, M.C. Wilson, M. Montal, Tyrosine phosphorylation modulates the activity of clostridial neurotoxins, J. Biol. Chem. 271 (1996) 18322–18325.
[16] Y.C. Tsai, R. Maditz, C. LingKuo, P.S. Fishman, C.B. Shoemaker, G.A. Oyler, A.M. Weissman, Targeting botulinum neurotoxin persistence by the ubiquitin- proteasome system, PNAS (2010) 1–6.
[17] R. Kukreja, B.R. Singh, Biologically active novel conformational state of botulinum, the most poisonous poison, J. Biol. Chem. 280 (2005) 39346–39352.
[18] L. Li, B.R. Singh, High level expression, purification and characterization of recombinant type A botulinum neurotoxin light chain, Protein Expr. Purif. 17 (1999) 339–344.
[19] J.T. Yang, C.S. Wu, H.M. Martinez, Calculation of protein conformation from circular dichroism, Methods Enzymol. 130 (1986) 208–269.
[20] S.M. Kelly, N.C. Price, The use of circular dichroism in the investigation of protein structure and function, Curr. Protein Pept. Sci. 1 (2000) 349–384.
[21] B.R. Singh, B.R. DasGupta, Changes in the molecular topography of the light and heavy chains of type A botulinum neurotoxin following their separation, Biophys. Chem. 34 (1989) 259–267.
[22] P.D.J. Moens, M.K. Helms, D.M. Jameson, Detection of tryptophan energy transfer in proteins, Protein J. 23 (2004) 79–83.
[23] R. Kumar, R. Kukreja, L. Li, A. Zhmurov, O. Kononova, S. Cai, S. Ahmed, V. Barsegov, B.R. Singh, Botulinum neurotoxin: unique folding of enzyme domain of the most poisonous poison, JBSD 2014 32 (2014) 804–815.
[24] S. Cai, B.R. Singh, Role of the disulfide cleavage induced molten globule state of type A botulinum neurotoxin in its endopeptidase activity, Biochemistry 40 (2001) 15327–15333.
[25] G. Schiavo, F. Benfenati, B. Poulain, O. Rossetto, P. Polverino de Laureto, B.R. DasGupta, C. Montecucco, Tetanus and botulinum-B neurotoxins block neurotransmitter release by proteolytic cleavage of synaptobrevin, Nature 359 (1992) 832–835.
[26] G. Schiavo, A. Santicci, B.R. DasGupta, P.P. Mehta, J. Jontes, F. Benfenati, M.C. Wilson, C. Montecucco, Botulinum neurotoxins serotypes A and E cleave SNAP-25 at distinct COOH-terminal peptide bonds, FEBS Lett. 335 (1993) 99–103.
[27] G. Schiavo, B. Poulain, F. Benfenati, B.R. DasGupta, C. Montecucco, Novel targets and catalytic activities of bacterial protein toxins, Trends Microbiol. 1 (1993) 170–174.
[28] G. Dayanithi, B. Stecher, B. Hohne-Zell, S. Yamasaki, T. Binz, U. Weller, H. Niemann, M. Gratzi, Exploring the functional domain and target of the tetanus toxin light chain in neurohypophysical terminals, Neuroscience 58 (1994) 423–431.
[29] M.A. Breidenbach, A.T. Brunger, Substrate recognition strategy for botulinum neurtoxin serotype A, Nature 432 (2004) 925–929.
[30] M. Ohgushi, A. Wada, Molten-globule state: a compact form of globular proteins with mobile side-chains, FEBS lett. 161 (1983) 21–24.
[31] R.V. Kukreja, S.K. Sharma, B.R. Singh, Molecular basis of activation of endopeptidase activity of botulinum neurotoxin type E, Biochemistry 49 (2010) 2510–2519.
[32] V.S. Pande, D.S. Rokhsar, Is the molten globule a third phase of proteins? PNAS 95 (1998) 1490–1494.
[33] L. Regan, Molten globules move into action, PNAS 100 (2003) 3553–3554.
[34] Y. Kuroda, S. Kidokoro, A. Wada, Thermodynamic characterization of cytochrome c at low pH: observation of the molten globule state and of the cold denaturation process, J. Mol. Biol. 20 (1992) 1139–1153.
[35] J.J. Ewbank, T.E. Creighton, The molten globule protein conformation probed by disulphide bonds, Nature 350 (1991) 518–520.
[36] A.F. Chaffotte, J.I. Gujjarro, Y. Gujllo, M. Delepierre, M.E. Goldberg, The "pre-molten globule," a new intermediate in protein folding, J. Protein Chem. 16 (1997) 433–439.
[37] S. Samaddar, A.K. Mandal, S.K. Mondal, K. Sahu, K. Bhattacharyya, S. Roy, Solvent dynamics of a protein in the pre-molten globule state, J. Phys. Chem. B 110 (2006) 21210–21215.